The decreasing albedo of the Zhadang glacier on western Nyainqentanglha and the role of light-absorbing impurities

B. Qu[4,1], J. Ming[1,2,3], S.-C. Kang[1,4], G.-S. Zhang[4], Y.-W. Li[4], C.-D. Li[4], S.-Y. Zhao[5], Z.-M. Ji[4], and J.-J Cao[5]

1 State Key Laboratory of Cryospheric Sciences, Cold and Arid Regions Environmental and Engineering Research Institute, Chinese Academy of Sciences, Lanzhou, China

2 Collaborative Innovation Centre on Forecast and Evaluation of Meteorological Disasters，Nanjing University of Information Science & Technology, Nanjing, China

3 National Climate Centre, China Meteorological Administration (CMA), Beijing, China

4 Key Laboratory of Tibetan Environment Changes and Land surface Processes, Institute of Tibetan Plateau Research, Chinese Academy of Sciences, Beijing, China

5 State Key Laboratory of Loess and Quaternary Geology, Institute of Earth Environment, Chinese Academy of Sciences, Xi’an, China

Corresponding author: J. Ming (petermingjing@hotmail.com)

Abstract

A large change in albedo has a significant effect on glacier ablation. Atmospheric aerosols (e.g., black carbon (BC) and dust) can reduce the albedo of glaciers and thus contribute to their melting. In this study, two main themes were explored, 1) the decrease in albedo of the Zhadang glacier on Mt. Nyainqentanglha between 2001 and 2012, as observed by the Moderate Resolution Imaging Spectroradiometer (MODIS) on-board the Terra satellite, and the correlation of this albedo with mass balance; and 2) the concentrations of BC and dust in the glacier measured during 2012, and the associated impacts of these impurities on albedo and radiative forcings (RF). The average albedo of the Zhadang glacier from the MODIS increased with the altitude and fluctuated but had a decreasing trend during the period 2001–2012, with the highest (0.722) in 2003 and the lowest (0.597) in 2009 and 2010. The mass balance of the glacier has a positively significant correlation with its surface albedo derived from MODIS. Snow samples were collected on the Zhadang glacier to measure the BC and dust in the summer of 2012. The impacts of BC and dust on albedo reduction in different melting conditions were identified with the SNow ICe Aerosol Radiative (SNICAR) model initiated by in-situ observation data. The sensitivity analysis showed that BC was a major factor in albedo reduction when the glacier was covered by newly fallen snow. Nevertheless, the contribution of dust to albedo reduction can reach as high as 56%, much exceeding that of BC (28%), when the glacier experiences strong surficial melting and its surface was almost bare ice. The average RF caused by dust could increase from 1.1 to 8.6 W m^{-2}, exceeding the RF caused by BC after snow was deposited and surface melting occurred in the Zhadang glacier. This implies that it may be dust that primarily dominates the melting of some glaciers in the inner TP during melting seasons, rather than BC.

1. Introduction

Glaciers and snow cover are important reservoirs of fresh water on Earth. A rough volume of 2.4×10^7 km^3 of water is stored in them (Oki and Kanae, 2006), and changes in these reservoirs have a significant effect on the water supply in many regions of the world (Mote et al., 2003; Yao et al., 2012). The Tibetan Plateau (TP) is the source of many great rivers (e.g., Yangtze, Yellow, Indus, Ganges, and Brahmaputra rivers), which concentrate their sources at the glaciers in the TP known as the "Asian Water Towers". More than 1.4 billion people depend on the water from these rivers (Immerzeel et al., 2010), but these glaciers have been undergoing rapid changes (Kang et al., 2010; Yao et al., 2012). Therefore, it is important to understand the impact factors that affect the glaciers and snow cover.

The surface energy budget of glaciers has significant effects on their ablation (Zhang et al., 2013), and snow/ice albedo is one of the most important parameters that affect the absorbed radiation. Snow/ice albedo is defined as the fraction of the reflected and the incident radiant flux in the surface of the snow/ice. A higher albedo implies a cleaner snow surface or less energy available for melting. Clean snow has the highest albedo (as high as 0.9) of any natural substance, but this diminishes when the snow surface is dirty or darkened due to snow grain size increases (Warren and Wiscombe, 1980; Wiscombe and Warren, 1980). A recent report (Lhermitte et al., 2012) indicates a darkening surface of the Greenland ice sheet and a rapidly decreasing albedo during 2000–2011, which will greatly increase the rate of mass loss of the ice sheet as more solar energy is absorbed by the darker glacial ice (Farmer and Cook, 2013).

Temperature, precipitation, and glacial dynamic processes are the key factors that affect glacial change (Sugden and John, 1976). However, there is now a general consensus that light-absorbing constituents (LACs, e.g., black carbon (BC) and dust) can reduce the albedo of glaciers (dirtying or darkening effect) and thus also contribute to the mass loss of glaciers. Both BC and dust are important absorbers of solar radiation in the visible spectrum (Warren and Wiscombe, 1980; Hadley and Kirchstetter, 2012; IPCC, 2007), and BC has an absorbing capacity approximately 50 to 200 times greater than dust (Warren and Wiscombe, 1980). The impacts of BC and dust deposited on the TP glaciers (in particular, on their radiation balance) have been reported in previous literature (Xu et al., 2006; Ming et al., 2009a, 2013a; Lau et al., 2010; Qian et al., 2011). Simulation of the effect of LACs on the albedo of Himalayan glaciers showed that LACs in this region had a contribution of 34% to the albedo reduction during the late spring time, with 21% due to BC and 13% originating from dust (Ming et al., 2012).

The lowering of the surface albedo due to the presence of a dust layer could also lead to a drastic increase in the glacier melting rate during the melting season (Fujita, 2007). In general, BC can be transported over long distances (Ming et al., 2010; Cao et al., 2010; Kopacz et al., 2011), whereas dust usually comes from the local or regional environment of the glaciers (Kang et al., 2000). Historical deposition records of BC revealed by ice cores and lake sediments over the TP indicate that BC originating from south and central Asia has reached the glaciers in recent decades (Ming et al., 2008; Xu et al., 2009b; Cong et al., 2013; Wang et al., 2014).

There has been extensive research focusing on quantifying the impact of LACs in ice cores and snow cover to understand the relationship between LACs and albedo reduction (Aoki et al., 2011; Painter et al., 2007, 2012; Ginot et al., 2013; Kaspari et al., 2013). However, few researchers discussed the exact effects that BC and dust have on different types of glacier surfaces during the melting season. Dust sometimes causes significant spatial variation of the surface albedo in glaciers. Moreover, glacier melting causes LAC particles to concentrate in the surface and to further enhance the absorption of radiation. This positive feedback highlights the importance of investigating LACs and their effects on the albedo and glacial melt across a whole glacier, particularly in the background that the global glaciers are shrinking in general (IPCC, 2007) and the total BC emission is increasing (Bond et al., 2013).

The glaciers in the mid Himalaya have been in general darkening since 2000, which is partly attributed to the deposition of LACs, revealed by a previous study (Ming et al., 2012). Whereas, the Zhadang glacier in the inner TP showed a mass balance of -1500 mm water equivalent in 2005-2006 (Zhou et al., 2007), experiencing much stronger melting than Himalayan glaciers. Albedo and the factors inducing the variation of albedo are the “footstone” for understanding the dramatic change of the glaciers. Neither the long-term variation of the albedo of the Zhadang glacier, nor the impact of LACs on the albedo has been previously studied.

In this work, we will firstly investigate the albedo variation of the Zhadang glacier derived from the Moderate Resolution Imaging Spectroradiometer (MODIS) on-board the Terra satellite from 2001 through 2012, and then discuss the spatial distribution of LACs from the terminate along to the accumulation zone of the Zhadang glacier during the summer of 2012, and last estimate the contribution of BC and dust to the albedo reduction in different melting conditions by simulations.

2. Methodology

The Zhadang glacier is located in western Nyainqentanglha, southern TP, (30°28.57′N, 90°38.71′E, and 5500-5800 m a.s.l.) (Fig. 1). Surface snow/ice samples were collected, and the surface albedo was observed on the Zhadang glacier during 12-16 July and 24-27 August, 2012. The observation of surface mass balance on the Zhadang glacier has been conducted by the traditional stake method since late 2005 (Zhou et al., 2007).

We classified three conditions or scenarios of the glacier surface: (1) S-I: the surface of the glacier is bare ice containing some visible dark constituents (Fig. 2a); (2) S-II: the surface is covered by aged snow/firn (Fig. 2a); (3) S-III: the surface is covered by fresh snow (Fig. 2b). These surface conditions are typical in most alpine glaciers throughout the year (Benn and Evans, 2010). A description of the sampling details in the Zhadang glacier is given in Table 1.

2.1 Albedo data from the MODIS

The MODIS albedo data were used to investigate the albedo change in the Zhadang glacier. The series of the product is the MODIS/Terra Snow Cover Daily L3 Global 500m Grid (MOD10A1), which is based on a snow mapping algorithm that employs a normalised difference snow index (NDSI) and other criteria tests (Riggs and Hall, 2011). The MOD10A1 product contains four data layers: snow cover, snow albedo, fractional snow cover, and binary quality assessment (QA), which is assigned as “good” or “bad”. The data are compressed in hierarchical data format-Earth observing system (HDF-EOS) and are formatted along with the corresponding metadata. The images of MOD10A1 are 1200 km by 1200 km tiles with a resolution of 500 m × 500 m gridded in a sinusoidal map projection. Data are available from 24 February 2000 to present via FTP (Hall et al., 2006). The snow albedo data used in the calculation are based on three expected criteria: the pixels are identified as snow cover, fractional snow cover is 100, and the pixels pass the QA. The MODIS daily albedo has high accuracy in flat terrain (Stroeve et al., 2006; Tekeli et al., 2006.), but it shows some errors in complex topography, such as mountainous regions (Sorman et al., 2007; Warren, 2013).

To verify the applicability of the MOD10A1 product in the Zhadang glacier, we used the observed data measured by the Kipp & Zonen radiometers mounted on an automatic weather station (AWS) that was set in the saddle of the glacier (5680 m a.s.l., Fig. 1). The albedo data were extracted from the precise pixel in the relevant MODIS image where the AWS was located. The observed albedos were selected in the local time period of 12:30 to 13:30 LT, considering the scanning time of the Terra satellite passing over the study area. The correlation analysis between the MODIS data and the observed data showed a good relationship at the confidence level of 0.02 (Fig. 3), indicating that it is reasonable to use MOD10A1 data to study the albedo change of the Zhadang glacier.

2.2 Field albedo observation

Warren (2013) suggested that it is unlikely to detect the impact of BC on snow albedo by remote sensing. In this work, a spectroradiometer (Model ASD$^{®}$ FS-3) was used to measure the spectral albedo of the glacier. This covers a radiation waveband of 350-2500 nm with a wavelength resolution of one nanometre. The optical sensor of the spectroradiometer was set in a pistol-shape device so that the optical fibre can be fixed inside and mounted on the rocker arm of the tripod with a gradienter for levelling. The distance between the sensor and the snow surface was approximately 0.5 m, allowing for the measurement of the spectral reflectances. Air temperature has been recorded by an autonomous weather station (AWS) built up in the accumulative zone of the Zhadang glacier since 2008 (Fig. 1).

During the expedition of July 2012, we measured the surface albedo and collected snow samples in S-I (two sites: A and B) and S-II (C and D) conditions. In August, the glacier was covered by newly fallen snow, and the albedo and surface snow samples were successfully observed and collected at eight sites in S-III conditions (Fig. 2). Along with the sampling, other necessary parameters, such as snow density, and grain sizes, for simulating the surface albedo were also observed. Details concerning the simulations of the surface albedo have been introduced in a previous work (Ming et al., 2013a).

2.3 Snow/ice sampling and BC/dust measurement

Snow/ice samples were collected in accordance with the "Clean Hands-Dirty Hands" principle, meaning that the person whose hands are collecting sampling will not touch any other material that may contaminate the snow samples (Fitzgerald, 1999). We collected two parallel samples 10 cm away from each other from the surface to 5 cm depth at each site when measuring the albedo. The snow density was measured using a balance. The samples were stored in NALGENE® HDPE wide-mouth bottles (250 mL) and were kept frozen until laboratory analysis. The snow grain sizes were measured using a hand lens (25X) with an accuracy of 0.02 mm; the largest length of a single ice crystal was also measured using a snow crystal card with 1 mm grids (Aoki et al., 2007). We filtered the snow melt water through quartz-fibre filters, which were weighed before and after the filtration using a microbalance to evaluate the mass of on-load dust. A thermal-optical method of carbon analysis, using DRI® Model 2001A OC/EC (Chow et al., 1993), was employed to measure the BC mass in the samples.

2.4 Albedo reduction modelling and radiative forcing (RF)

The Snow-Ice-Aerosol-Radiative (SNICAR) model can be used to simulate the hemisphere albedo of snow and ice for unique combinations of impurity contents (BC, dust, and volcanic ash), snow grain size, and incident solar flux characteristics (Flanner et al., 2007). It was applied to simulate the albedo variation caused by BC and dust deposited in the glacier surface in this work. We conducted a series of sensitivity analyses to identify the impact of BC and dust on albedo reduction in three different surface conditions of the Zhadang glacier (also see Section 2.2). The solar zenith angle was identified based on the time and position of the specific sampling sites. The snow grain effective radius is taken as half the observed snow grain size introduced by Aoki et al. (2007) and is shown in Table 1. The albedo of the underlying bare ice is taken as 0.11-0.19 in the visible band and 0.18-0.23 in the near-infrared band as measured in-situ by the spectroradiometer. We use the default value 1 as the mass absorption cross section (MAC) scaling factor (experimental) in the modelling. The detailed parameters used in SNICAR are listed in the appendix.

RF was defined using the equation below,

$$RF = R_{in\text{–}short} * \Delta\alpha,$$

where $R_{in\text{-}short}$ denotes the incident solar radiation measured by radiometer, and $\Delta\alpha$ denotes the reduction of the albedo.

3. Results and Discussion

3.1 Surface albedo variations of the Zhadang glacier during the period 2001-2012

The albedo of the Zhadang glacier increased with elevation (Table 1) due to the lower temperature favouring more cold snow stored in higher elevations. The annual average albedo from the MODIS decreased from 0.676 in 2001 to 0.597 in 2010 with a maximum of 0.722 in 2003 and a minimum of 0.597 in 2009 and 2010. The albedo of the Zhadang glacier shows an obvious decreasing trend of 0.003 a^{-1} during the period 2001-2012, despite the inter-annual fluctuations (Fig. 4). This trend was also revealed in the Himalayan and Tanggula glaciers (Ming et al., 2012; Wang et al., 2012). Regional air temperature shows a decreasing trend during the period 2008-2012, which seems not to be the cause of the albedo decreasing (Fig. 4), implying that other factors could induce the varying.

The surface albedo of a specific glacier could be linked with its mass balance in the TP, which has been proved by Wang et al. (2013). We used the observed mass balance data from 2006 through 2012 in the Zhadang glacier (Zhou et al., 2007; Zhang et al., 2013) to perform a correlation analysis with the glacier surface albedo (Fig. 4). Lower albedos are related to more negative mass balances, and vice versa. For example, the most negative mass balance appeared in 2010 when the albedo reached the minimum, whereas the most positive mass balance occurred in 2008, and the albedo was also the highest. The significant positive correlation (n = 7, α = 0.01, $R^2 > 0.83$) between the albedo and the mass balance of the glacier implies that surface albedo is a strong index of the mass balance for the glacier.

3.2 Impacts of BC and dust on the albedo

A previous study conducted at a site approximately 20 km northeast of the Zhadang glacier indicated that the BC concentration showed an increasing trend during the period 2006-2010 (Zhao et al., 2013), which allows to presume the possibly increasing deposition of BC in the glacier surface, enhancing the surficial radiation absorption and decreasing the albedo. Thus taking LACs into consideration, and sampling and measuring their concentrations are reasonable for interpreting the albedo decreasing revealed by the MODIS data.

The measurements of BC and dust concentrations, as well as other observations, such as snow grain size, snowpack density, and snowpack thickness, on the Zhadang glacier are shown in Table 1. In S-I conditions, the concentration of dust varied from 504–1892 ppm with an average of 1198 ppm, whereas BC was 334–473 ppb with an average of 404 ppb. In S-II conditions, the concentrations of BC and dust ranged from 81 to 143 ppb with an average of 112 ppb and from 34 to 67 ppm with an average of 50 ppm, respectively. However, the concentration of BC in S-III was 41 to 59 ppb with an average of 52 ppb, whereas the dust concentration was 3 to 8 ppm with an average of 6 ppm.

There are large differences in the BC and dust concentrations in the surface of the Zhadang glacier in different scenarios of surface features (Fig. 2a). In S-I and S-II, intensive surface melting could lead to a strong enrichment of LACs in the surface of the glacier. In S-III conditions, the Zhadang glacier was covered by fresh snow due to frequent snowfalls at night (Fig. 2b). Thus, the concentrations of LACs in S-III are several magnitudes lower than those in S-I and S-II conditions (Table 1). Table 2 provides observed and simulated albedos at the sampling sites. The observed surface albedo increases roughly along with the elevation on the Zhadang glacier, in contrast with the concentrations of BC and dust in S-I and S-II conditions. The correlations of in-situ observed albedo and the albedo simulated by SNICAR after adding measured BC and dust into the snow surface are 0.9992 for S-I, 0.9995 for S-II, and 0.4729 for S-III, respectively. This implies that the enrichment of BC and dust on the surface of the glacier could reduce the glacier albedo, thus resulting in the melting of glaciers.

The sensitivity analysis of the respective impacts of BC and dust on reducing the snow albedo of the Zhadang glacier was calculated by SNICAR and is shown in Fig. 5. We assume that the model also works well for thin snow (< 5 cm) with ice beneath. This configuration with the SNICAR model implies that impurities contained within the ice beneath the snow do not contribute to the RF calculations. It is unclear how important this assumption is, but it may contribute to a low bias in the RF estimates. We presume three impacting factors dominating the albedo varying in the glacial surface, i.e., BC, dust, and the grain size growing due to warming (Ming et al., 2012). Dust exceeding BC was the most dominant factor in reducing glacier albedo in S-I. BC other than dust dominates albedo reduction in cases where the glacier was covered by snow (S-II and S-III). The incoming solar irradiances at every sampling time during the two trips are listed in Table 2.

We calculated the RF of both BC and dust on the Zhadang glacier. The simulation shows that the RF caused by BC and dust deposition on the Zhadang glacier varied between 0.4–11.8 W m^{-2} and 0.5–16.4 W m^{-2}, respectively (Fig. 5). The RF of dust is much higher than that of BC in S-I, whereas the RF of BC exceeds dust in S-II and S-III. On average, the forcing caused by dust deposition on the Zhadang glacier in the summer of 2012 was 2.7±3.4 W m^{-2}, and that caused by BC was 4.8±3.2 W m^{-2}, which is lower than that reported in the northern TP (Ming et al., 2013b) and higher than reported in the Arctic (Flanner, 2013; Dou et al., 2012). Lacking long-term measurements of LACs in the Zhadang glacier makes directly evaluating the impacts of LACs on the albedo decreasing in 2001-2012 impossible, whereas the investigation in 2012 presented a possible interpretation that the LACs could decrease the surface albedo, taking into consideration the increasing of BC concentration in surrounding atmosphere (Zhao et al., 2013).

4. Summary and Conclusions

The albedo of the Zhadang glacier decreased at the rate of -0.003 a^{-1} throughout 2001 to 2012, according to the MODIS data. The variation of albedo had a positively significant correlation with the mass-balance variation in 2006-2012, implying that remotely sensed albedo can be used as an indicating index of the mass balance of the glacier. The deposition of LACs may cause the decreasing of albedo in the Zhadang glacier while the surface temperature showed a decreasing trend. During the summer of 2012, the average concentrations of BC and dust were 404 ppb and 1198 ppm in the surface, which are one and three magnitudes higher than the 52 ppb of BC and the 6.4 ppm of dust in fresh snow of the Zhadang glacier. The impacts of BC and dust on the glacier albedo were quantified based on the observations and simulation. The contribution of dust and BC to albedo reduction was 56% and 28%, respectively, when the glacier was covered by bare ice. In the surface covered by aged snow, 36% of the surface albedo reduction was caused by BC, and 29% by dust. When the glacier was covered by fresh snow, BC and dust contributed 11% and 3% to albedo reduction, respectively. In general, BC is a major factor in albedo reduction when the glacier is covered by fresh and aged snow; however, dust makes the most significant contribution to albedo reduction when the surface of the glacier is bare ice.

Acknowledgements

This work was supported by the Global Change Research Program of China (2010CB951401), the National Natural Science Foundation of China (NSFC Grants 41121001), the State Key Laboratory of Cryospheric Sciences, CAS (no. SKLCS-ZZ-2012-01-06), CMA (no. GYHY201106023), the National Science & Technology Pillar Program during the Twelfth Five-year Plan Period (2012BAC20B05), the Climate Change Science Foundation of CMA (2013-2014), and the NSFC (Grants 41225002 and 41190081). We would like to thank H. Zhang for processing the albedo data and appreciate two anonymous referees for their constructive comments.

References

Aoki, T., Hori, M., Motoyoshi, H., Tanikawa, T., Hachikubo, A., Sugiura, K., Yasunari, T. J., Storvold, R., Eide, H. A., and Stamnes, K.: ADEOS-II/GLI snow/ice products—Part II: Validation results using GLI and MODIS data, Remote Sensing of Environment, 111, 274-290, 10.1016/j.rse.2007.02.035, 2007.

Aoki, T., Kuchiki, K., Niwano, M., Kodama, Y., Hosaka, M., and Tanaka, T.: Physically based snow albedo model for calculating broadband albedos and the solar heating profile in snowpack for general circulation models, Journal of Geophysical Research: Atmospheres (1984–2012), 116, 2011.

Benn, D. I., and Evans, D. J.: Glaciers and glaciation, Hodder Education, 2010.

Bond, T., Doherty, S., Fahey, D., Forster, P., Berntsen, T., DeAngelo, B., Flanner, M., Ghan, S., Kärcher, B., and Koch, D.: Bounding the role of black carbon in the climate system: A scientific assessment, Journal of Geophysical Research: Atmospheres, 10.1002/jgrd.50171, 2013.

Cao, J., Tie, X., Xu, B., Zhao, Z., Zhu, C., Li, G., and Liu, S.: Measuring and modeling black carbon (BC) contamination in the SE Tibetan Plateau, Journal of Atmospheric Chemistry. 67(1), 45-60, 2010.

Chow, J. C., Watson, J. G., Pritchett, L. C., Pierson, W. R., Frazier, C. A., and Purcell, R. G.: The DRI thermal/optical reflectance carbon analysis system: description, evaluation and applications in US air quality studies, Atmospheric Environment. Part A. General Topics, 27, 1185-1201, 1993.

Cong, Z., Kang, S., Gao, S., Zhang, Y., Li, Q., and Kawamura, K.: Historical trends of atmospheric black carbon on Tibetan Plateau as reconstructed from a 150-year lake sediment record, Environmental science & technology, 47(6), 2579-2586, 2013.

Dou, T., Xiao, C., Shindell, D., Liu, J., Eleftheriadis, K., Ming, J., and Qin, D.: The distribution of snow black carbon observed in the Arctic and compared to the GISS-PUCCINI model, Atmospheric Chemistry and Physics, 12, 7995-8007, 2012.

Farmer, G. T., and Cook, J.: Earth’s Albedo, Radiative Forcing and Climate Change, in: Climate Change Science: A Modern Synthesis, Springer, 217-229, 2013.

Fitzgerald, W. F.: Clean hands, dirty hands: Clair Patterson and the aquatic biogeochemistry of mercury, Clean Hands, Clair Patterson’s Crusade Against Environmental Lead Contamination, 119-137, 1999.

Flanner, M. G., Zender, C. S., Randerson, J. T., and Rasch, P. J.: Present-day climate forcing and response from black carbon in snow, J. Geophys. Res, 112, D11202, 10.1029/2006JD008003, 2007.

Flanner, M. G.: Arctic climate sensitivity to local black carbon, Journal of Geophysical Research: Atmospheres, 10.1002/jgrd.50176, 2013.

Fujita, K.: Effect of dust event timing on glacier runoff: sensitivity analysis for a Tibetan glacier, Hydrological Processes, 21, 2892-2896, 2007.

Ginot, P., Dumont, M., Lim, S., Patris, N., Taupin, J., Wagnon, P., Gilbert, A., Arnaud, Y., Marinoni, A., and Bonasoni, P.: A 10 yr record of black carbon and dust from Mera Peak ice core (Nepal): variability and potential impact on Himalayan glacier melting, Cryosphere

Discussions, 7, 2013.

Hall, Dorothy K., George A. Riggs, and Vincent V. Salomonson. MODIS/Terra Snow Cover Daily L3 Global 500m Grid V005, [January 2001 to December 2010]. Boulder, Colorado USA: National Snow and Ice Data Centre. Digital media (updated daily), 2006

Immerzeel, W. W., van Beek, L. P., and Bierkens, M. F.: Climate change will affect the Asian water towers, Science, 328, 1382-1385, 2010.

IPCC, C. C.: The Physical Science Basis. Contribution of Working Group I to the Fourth Assessment Report of the Intergovernmental Panel on Climate Change, Cambridge University Press, Cambridge, United Kingdom and New York, NY, USA, 996, 2007, 2007.

Kang, S., Wake, C. P., Dahe, Q., Mayewski, P. A., and Tandong, Y.: Monsoon and dust signals recorded in Dasuopu glacier, Tibetan Plateau, Journal of Glaciology, 46, 222-226, 2000.

Kang, S., Xu, Y., You, Q., Flügel, W. A., Pepin, N., and Yao, T.: Review of climate and cryospheric change in the Tibetan Plateau, Environmental Research Letters, 5, 015101, 2010.

Kaspari, S., Painter, T., Gysel, M., and Schwikowski, M.: Seasonal and elevational variations of black carbon and dust in snow and ice in the Solu-Khumbu, Nepal and estimated radiative forcings, Atmospheric Chemistry and Physics Discussions, 13, 33491-33521, 2013.

Kopacz, M., Mauzerall, D., Wang, J., Leibensperger, E., Henze, D., and K. Singh: Origin and radiative forcing of black carbon transported to the Himalayas and Tibetan Plateau, Atmospheric Chemistry and Physics. 11(6), 2837-2852, 2011.

Lau, W., Kim, M., Kim, K., and W. Lee: Enhanced surface warming and accelerated snow melt in the Himalayas and Tibetan Plateau induced by absorbing aerosols, Environmental Research Letters, 5(2), 2010.

Lhermitte, S., Greuell, W., van Meijgaard, E., van Oss, R., van den Broeke, M., and van de Berg, W.: Greenland ice sheet surface albedo: trends in surface properties (2000-2011), EGU General Assembly Conference Abstracts, 2012, 12349.

Ming, J., Cachier, H., Xiao, C., Qin, D., Kang, S., Hou, S., and Xu, J.: Black carbon record based on a shallow Himalayan ice core and its climatic implications, Atmospheric Chemistry and Physics, 8, 1352, 2008.

Ming, J., Xiao, C., Du, Z., and Flanner, M. G.: Black Carbon in snow/ice of west China and its radiave forcing, Advances in Climate Change Research, 92, 114-123, 2009a.

Ming, J., Xiao, C. D., Cachier, H., Qin, D. H., Qin, X., Li, Z. Q., and Pu, J. C.: Black Carbon (BC) in the snow of glaciers in west China and its potential effects on albedos, Atmospheric Research, 92, 114-123, 2009b.

Ming, J., Xiao, C., Sun, J., Kang, S., and Bonasoni, P.: Carbonaceous particles in the atmosphere and precipitation of the Nam Co region, central Tibet, Journal of Environmental Sciences, 22, 1748-1756, 2010.

Ming, J., Du, Z., Xiao, C., Xu, X., and Zhang, D.: Darkening of the mid-Himalaya glaciers since 2000 and the potential causes, Environmental Research Letters, 7, 014021, 2012.

Ming, J., Wang, P., Zhao, S., and Chen, P.: Disturbance of light-absorbing aerosols on the albedo in a winter snowpack of Central Tibet, Journal of Environmental Sciences, 337, 2013a.

Ming, J., Xiao, C., Du, Z., and Yang, X.: An Overview of Black Carbon Deposition in High Asia Glaciers and its Impacts on Radiation Balance, Advances in Water Resources, 80-87, 2013b.

Mote, P. W., Parson, E. A., Hamlet, A. F., Keeton, W. S., Lettenmaier, D., Mantua, N., Miles, E. L., Peterson, D. W., Peterson, D. L., and Slaughter, R.: Preparing for climatic change: the water, salmon, and forests of the Pacific Northwest, Climatic Change, 61, 45-88, 2003.

Oki, T., and Kanae, S.: Global hydrological cycles and world water resources, science, 313, 1068-1072, 2006.

Painter, T. H., Barrett, A. P., Landry, C. C., Neff, J. C., Cassidy, M. P., Lawrence, C. R., McBride, K. E., and Farmer, G. L.: Impact of disturbed desert soils on duration of mountain snow cover, Geophysical Research Letters, 34, 2007.

Painter, T. H., Skiles, S. M., Deems, J. S., Bryant, A. C., and Landry, C. C.: Dust radiative forcing in snow of the Upper Colorado River Basin: 1. A 6 year record of energy balance, radiation, and dust concentrations, Water Resources Research, 48, 2012.

Qian, Y., Flanner, M., Leung, L., and Wang, W.: Sensitivity studies on the impacts of Tibetan Plateau snowpack pollution on the Asian hydrological cycle and monsoon climate, Atmospheric Chemistry and Physics, 11(5), 1929-1948, 2011.

Riggs G, Hall D: MODIS snow and ice products, and their assessment and applications, Land Remote Sensing and Global Environmental Change. Springer New York, 681-707, 2011.

Sorman, A., Akyürek, Z., Sensoy, A., Sorman, A., and Tekeli, A.: Commentary on comparison of MODIS snow cover and albedo products with ground observations over the mountainous terrain of Turkey, Hydrol. Earth Syst. Sci, 11, 1353-1360, 2007.

Stroeve, J. C., Box, J. E., and Haran, T.: Evaluation of the MODIS (MOD10A1) daily snow albedo product over the Greenland ice sheet, Remote Sensing of Environment, 105, 155-171, 2006.

Sugden, D. E., and John, B. S.: Glaciers and landscape: a geomorphological approach, Edward Arnold London, 1976.

Tekeli, A. E., Şensoy, A., Şorman, A., Akyürek, Z., and Şorman, Ü.: Accuracy assessment of MODIS daily snow albedo retrievals with in situ measurements in Karasu basin, Turkey, Hydrological processes, 20, 705-721, 2006.

Wang, M., Xu, B., Cao, J., Tie, X., Wang, H., Zhang, R., Qian, Y., Rasch, P. J., Zhao, S., Wu, G., Zhao, H., Joswiak, D. R., Li, J., and Xie, Y.: Carbonaceous aerosols recorded in a Southeastern Tibetan glacier: variations, sources and radiative forcing, Atmos. Chem. Phys. Discuss., 14, 19719-19746, 2014.

Wang, J., B. Ye, Y. Cui, X. He, and G. Yang: Spatial and temporal variations of albedo on nine glaciers in western China from 2000 to 2011, Hydrol Process., doi:10.1002/hyp.9883, 2013

Wang, Q., Jacob, D., Fisher, J., Mao, J., Leibensperger, E., Carouge, C., Sager, P., Kondo, Y., Jimenez, J., and Cubison, M.: Sources of carbonaceous aerosols and deposited black carbon in the Arctic in winter-spring: implications for radiative forcing, Atmospheric Chemistry and Physics, 11, 12453-12473, 2011.

Warren, S.G., Wiscombe, W.J. A model for the spectral albedo of snow. II: Snow containing atmospheric aerosols. J. Atmos. Sci 37, 2734-2745, 1980.

Warren, S. G.: Can black carbon in snow be detected by remote sensing?, Journal of Geophysical Research: Atmospheres, 118, 779-786, 2013.

Wiscombe, W.J., Warren, S.G. A model for the spectral albedo of snow. I: Pure snow. Journal of the atmospheric sciences 37, 2712-2733, 1980.

Xu, B., Yao, T., Liu, X., and Wang, N.: Elemental and organic carbon measurements with a two-step heating gas chromatography system in snow samples from the Tibetan Plateau, Ann. Glaciol., 43(1), 257-262, 2006.

Xu, B., Cao, J., Hansen, J., Yao, T., Joswia, D. R., Wang, N., Wu, G., Wang, M., Zhao, H., and Yang, W.: Black soot and the survival of Tibetan glaciers, Proceedings of the National Academy of Sciences, 106, 22114-22118, 2009a.

Xu, B., Wang, M., Joswiak, D. R., Cao, J. J., Yao, T. D., Wu, G. J., Yang, W., and Zhao, H. B.: Deposition of anthropogenic aerosols in a southeastern Tibetan glacier, J. Geophys. Res, 114, D17209, 10.1029/2008JD011510, 2009b.

Xu, B., Cao, J., Joswiak, D. R., Liu, X., Zhao, H., and He, J.: Post-depositional enrichment of black soot in snow-pack and accelerated melting of Tibetan glaciers, Environmental Research Letters, 7, 014022, 2012.

Yao, T., Thompson, L., Yang, W., Yu, W., Gao, Y., Guo, X., Yang, X., Duan, K., Zhao, H., and

Xu, B.: Different glacier status with atmospheric circulations in Tibetan Plateau and surroundings, Nature Climate Change, 2, 663-667, 2012.

Zhang, G., Kang, S., Fujita, K., Huintjes, E., Xu, J., Yamazaki, T., Haginoya, S., Wei, Y., Scherer, D., and Schneider, C.: Energy and mass balance of Zhadang glacier surface, central Tibetan Plateau, Journal of Glaciology, 59, 137-148, 2013.

Zhao, S., Ming, J., Sun, J., and Xiao, C.: Observation of carbonaceous aerosols during 2006-2009 in Nyainqentanglha Mountains and the implications for glaciers, Environmental Science and Pollution Research, 20(8), 5827-5838, 2013.

Zhou, G., Yao, T., Kang, S., Pu, J., Tian, L., and Yang, W.: Mass balance of the Zhadang glacier in the central Tibetan Plateau, Journal of Glaciology and Geocryology (Chinese with English abstract), 29(3), 360-365, 2007.

Table 1. Sampling information: Two expeditions were conducted on the Zhadang glacier, and samples (albedo, snow/ice) were collected under three melting conditions of the glacier in July and August of 2012. We measured the albedo five to six times at each site whilst collecting two to three snow/ice samples. In total, 120 albedo measurements and 48 snow/ice samples were obtained at the A - D sample sites in July, 2012 for the S-I and S-II conditions (Fig. 2). A total of 160 albedo samples and 64 snow samples were obtained at all sampling sites in August 2012. The albedo and concentrations of BC and dust are listed here.

Sample date	Sample site	Altitude (m a.s.l.)	Number of samples (albedo/ snow & ice)	Average of albedo	Average of BC conc. (ppb)	Average of dust conc. (ppm)	Snow grain size (mm)	Snowpack density (kg/m^3)	Snowpack Thickness (cm)	Solar zenith angle (°)	Cloud Amount (10=100%)	Scene type
July, 2012	A	5507	30/12	0.385	472.6	503.8	0.8 ~ 1.6	289 ~ 380	1	44.8~78.9	3~10	S-I
	B	5680	30/12	0.521	334.4	1891.9	0.6 ~ 1.6	289 ~ 350	1~2	52.3~75.8	1~10	
	C	5720	30/12	0.676	142.9	66.6	0.4 ~ 0.7	333 ~ 378	2~3	62.9~79.1	1~10	S-II
	D	5795	30/12	0.686	80.9	33.6	0.3 ~ 0.5	267~ 289	3	67.1~67.3	0~10	
August, 2012	A	5507	20/8	0.589	53.2	8.2	0.2 ~ 0.5	278 ~ 300	1~2	33.4~44	0~10	S-III
	B	5560	20/8	0.696	40.8	8.0	0.2 ~ 0.4	256 ~ 289	2~3	37.6~47.1	1~7	
	C	5626	20/8	0.710	55.5	7.0	0.2 ~ 0.4	267~ 311	2~3	40.8~50.2	0~7	
	D	5680	20/8	0.699	52.7	6.7	0.2 ~ 0.4	267~289	3	43.8~54.1	1~8	
	E	5695	20/8	0.708	55.2	6.4	0.2 ~ 0.4	267~289	3~4	45.8~57.9	0~6	
	F	5715	20/8	0.667	57.7	6.2	0.2 ~ 0.4	278~289	4	49.9~61.4	0~7	
	G	5750	20/8	0.698	59.4	5.2	0.2 ~ 0.3	222~244	5	51.9~64.6	0~7	
	H	5795	20/8	0.724	40.9	3.4	0.2 ~ 0.3	211~222	5	61.2~68.4	0~10	

Table 2. Sensitivity analysis with the SNICAR model. BC% and dust% are the contributions of BC and dust to the total reduction of the albedo, respectively. $R_{in\text{-}short}$ is the incident solar radiation measured by AWS.

Date	Site	OA*	SA** pure	SA +BC	SA +BC & dust	BC%	dust%	$R_{in\text{-}short}$	RF +BC	RF +dust	Scene type
15 July	A	0.385	0.406	0.395	0.388	52	33	780.1	8.6	5.5	S-I
16 July	A	0.387	0.413	0.405	0.396	31	34	412.6	3.3	3.7	
15 July	B	0.363	0.406	0.394	0.364	28	70	548.2	6.6	16.4	
16 July	B	0.558	0.577	0.576	0.560	4	85	535.3	0.4	8.6	
14 July	C	0.618	0.640	0.631	0.624	41	32	1308.5	11.8	9.2	S-II
15 July	C	0.723	0.758	0.742	0.727	46	43	543.7	8.7	8.2	
16 July	C	0.745	0.756	0.754	0.752	18	18	604.4	1.2	1.2	
14 July	D	0.745	0.771	0.760	0.753	42	27	552.7	6.1	3.9	
15 July	D	0.732	0.754	0.745	0.740	41	23	648.4	5.8	3.2	
16 July	D	0.755	0.775	0.770	0.764	25	30	789.8	3.9	4.7	
24 Aug	A	0.568	0.791	0.786	0.784	2	1	337.8	1.4	0.7	S-III
25 Aug	A	0.653	0.682	0.681	0.680	5	2	658.7	0.9	0.5	
26 Aug	A	0.716	0.746	0.739	0.737	23	7	702.5	4.9	1.4	
24 Aug	B	0.759	0.793	0.779	0.778	41	4	608.1	8.5	0.9	
25 Aug	B	0.696	0.731	0.728	0.727	8	4	722.7	1.9	0.9	
26 Aug	B	0.656	0.683	0.681	0.68	7	4	736.2	1.5	0.7	
26 Aug	C	0.697	0.734	0.732	0.732	5	1	776.8	1.6	0.3	
24 Aug	D	0.726	0.806	0.797	0.795	11	3	822.6	7.4	1.6	
25 Aug	D	0.768	0.781	0.780	0.778	17	10	814	1.8	1.1	
26 Aug	D	0.647	0.781	0.779	0.778	1	1	811	1.3	1.0	
24 Aug	E	0.699	0.810	0.803	0.802	6	1	962	6.7	1.0	
25 Aug	E	0.780	0.813	0.809	0.807	12	6	891.5	3.6	1.8	
26 Aug	E	0.774	0.811	0.805	0.804	16	3	831	5.0	1.0	
24 Aug	F	0.792	0.839	0.835	0.833	9	4	786.8	3.1	1.6	
25 Aug	F	0.790	0.819	0.816	0.815	10	3	1030	3.1	1.0	
26 Aug	F	0.566	0.816	0.809	0.808	3	1	895	6.0	1.2	
24 Aug	G	0.795	0.848	0.840	0.838	15	4	1303	10.4	2.6	
25 Aug	G	0.806	0.828	0.824	0.823	18	5	1168	4.7	1.2	
26 Aug	G	0.652	0.819	0.812	0.811	4	1	932	6.5	0.9	
24 Aug	H	0.811	0.853	0.846	0.846	16	1	1134	7.5	0.6	
25 Aug	H	0.809	0.834	0.831	0.830	12	4	1316	3.9	1.3	
26 Aug	H	0.711	0.827	0.825	0.824	2	1	1192	2.4	1.2	
Avg.	S-I,II,III	0.684	0.741	0.735	0.731	18	15	826.1	4.7	2.8	

* OA denotes observed albedo. ** SA denotes simulated albedo.

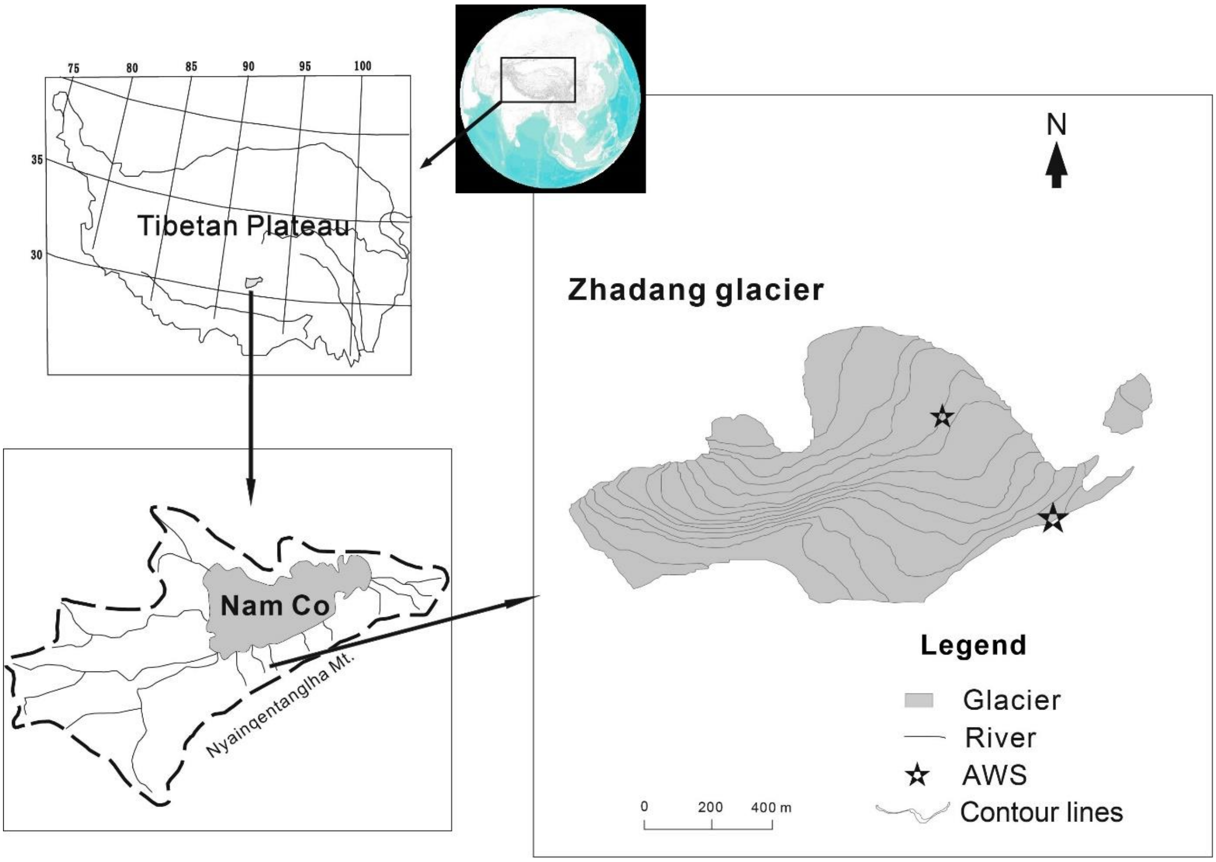

Fig. 1. Location of the Zhadang glacier on Mt. Nyainqentanglha.

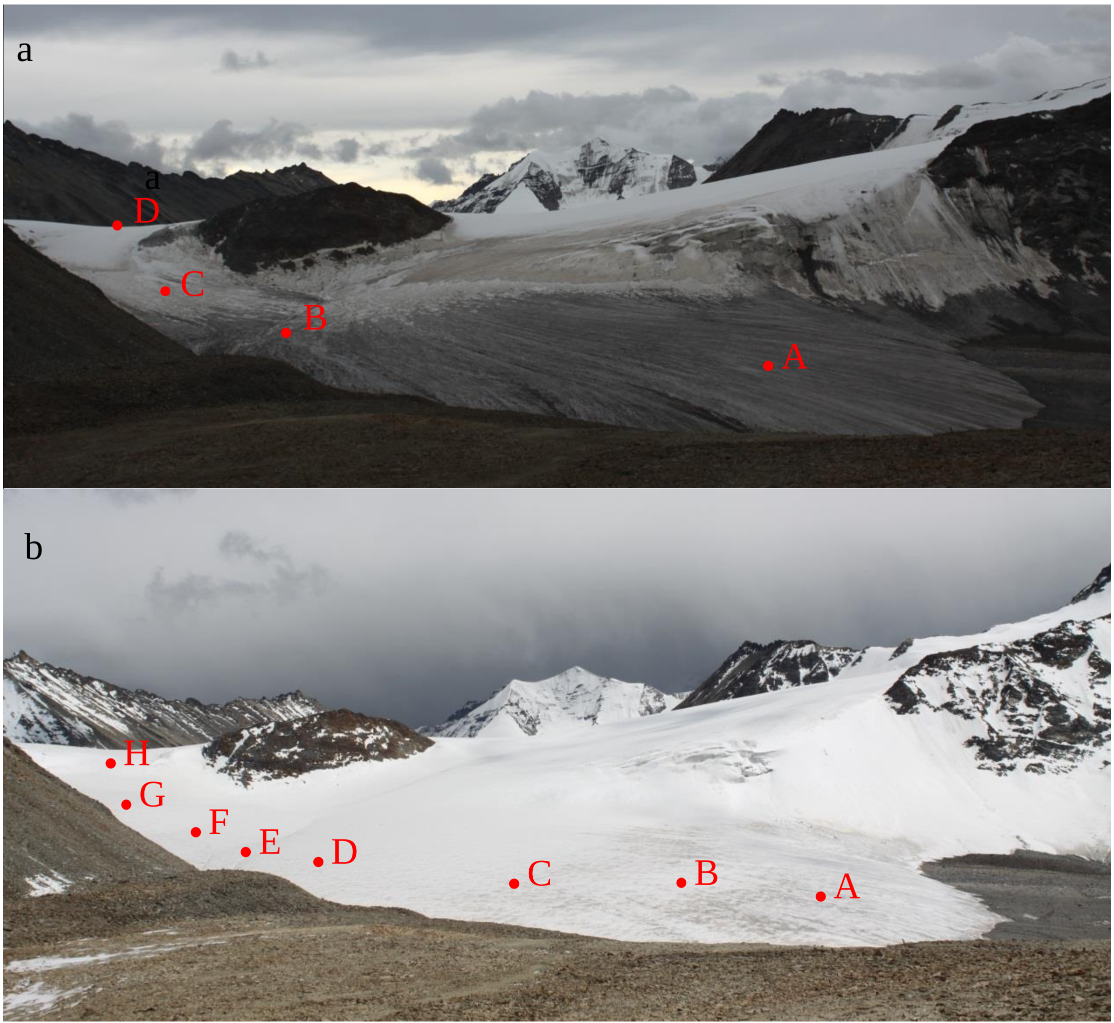

Fig. 2. Surface features of the Zhadang glacier on 16th Jul. (a) and 26th Aug. (b). The two surface conditions include three types of melting conditions: S-I: Sites A and B, which are located in the superimposed ice belt (Fig. 2a); S-II: Sites C and D, which are in the upper area of the glacier (Fig. 2a); S-III: All sites were covered by fresh snow (Fig. 2b).

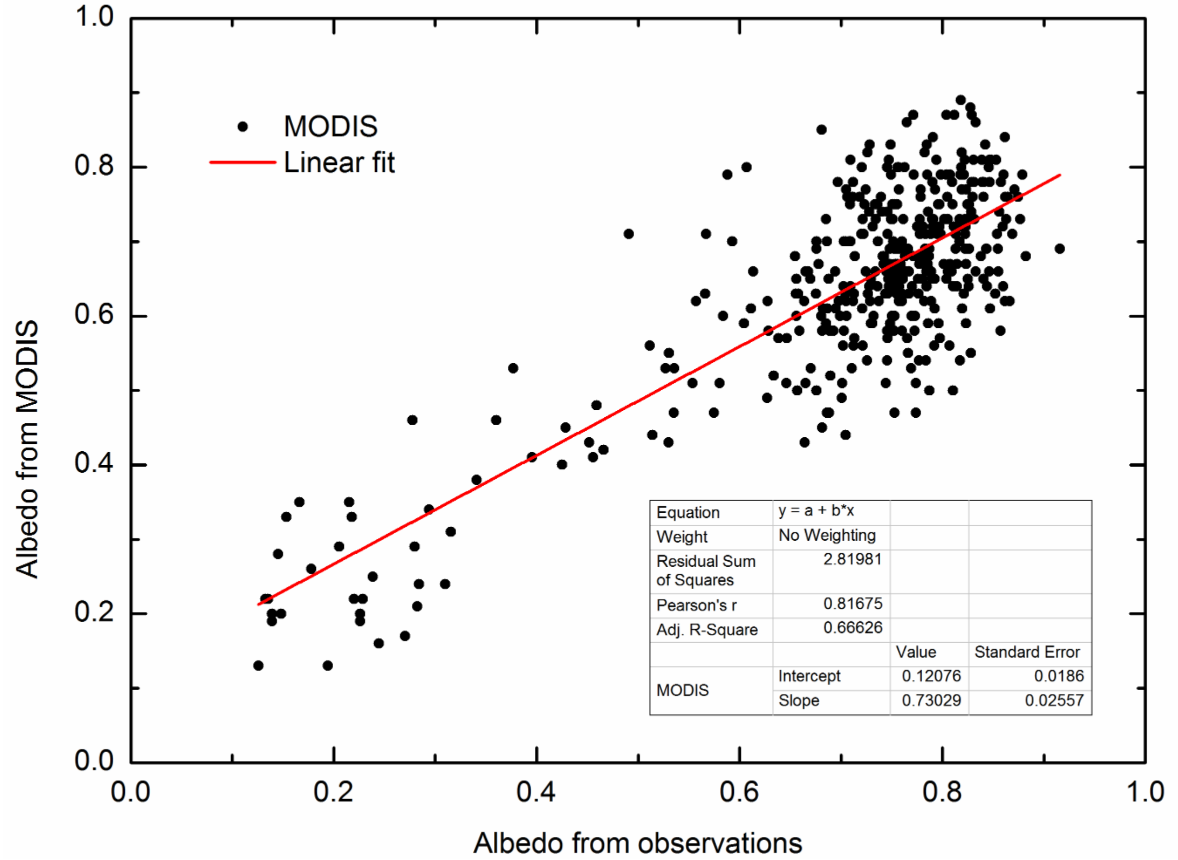

Equation	y = a + b*x		
Weight	No Weighting		
Residual Sum of Squares	2.81981		
Pearson's r	0.81675		
Adj. R-Square	0.66626		
		Value	Standard Error
MODIS	Intercept	0.12076	0.0186
	Slope	0.73029	0.02557

Fig. 3. The albedo of the pixel including the AWS in Zhadang glacier derived from MODIS and that observed by AWS in 2011.

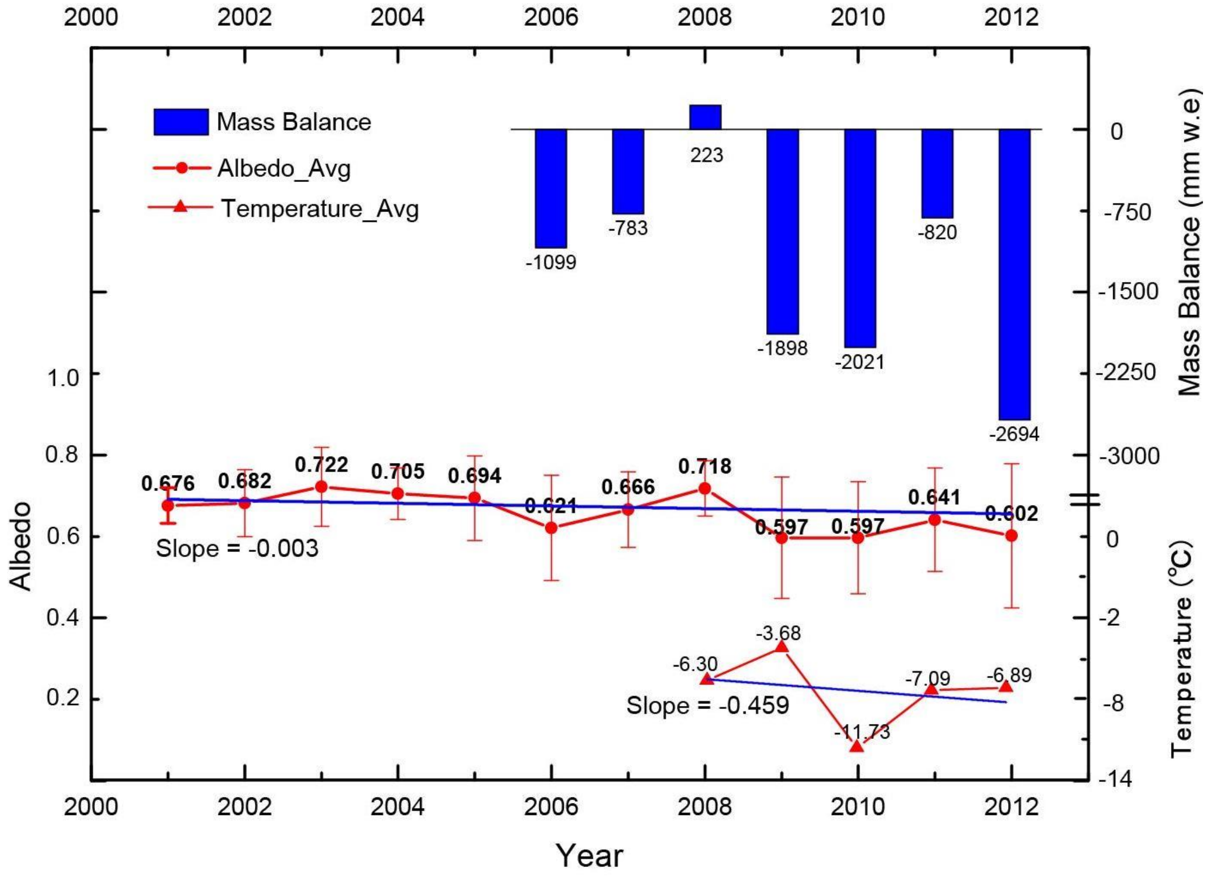

Fig. 4. Temporal changes of the albedo in the Zhadang glacier from 2001 to 2012 and the mass balance from 2006 to 2012. The albedo of the Zhadang glacier showed an overall downward trend in the last decade. Air temperature recorded by an AWS in the Zhadang glacier shows a slight decreasing trend.

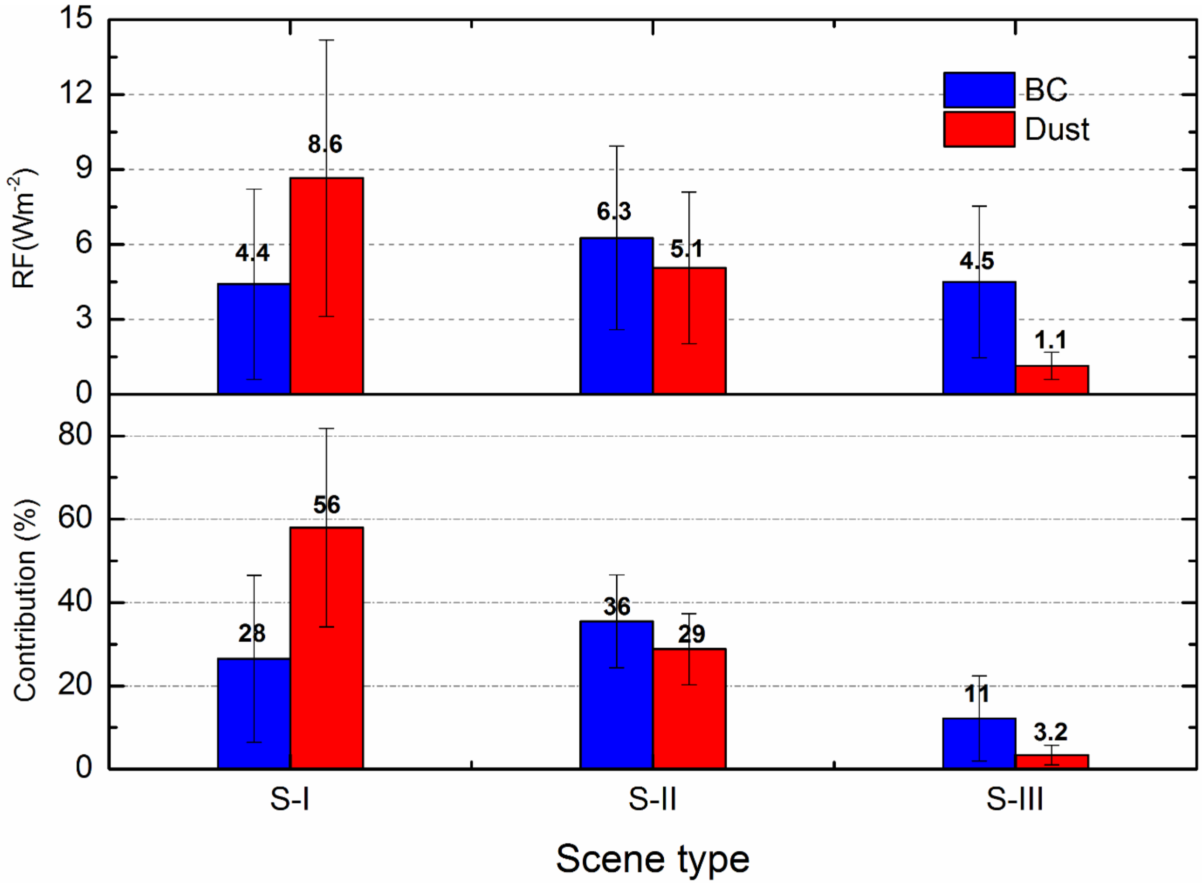

Fig. 5. Mid-day RFs of BC and dust on the Zhadang glacier and the contribution (results from the SNICAR model) show the reduction of the albedo in the surface snow cover area under three different melting conditions: S-I, where the surface of the glacier is bare ice; S-II, where the glacier is covered by aged snow; S-III, where the glacier is covered by fresh snow. Error bars show the uncertainties.

Appendix

Parameters for sensitivity analysis with SNICAR

1. Incident radiation (a. Direct, b. Diffuse); 2. Solar zenith angle; 3. Surface spectral distribution (a. Mid-latitude winter, clear-sky, cloud amount < 5. b. Mid-latitude winter, cloudy, cloud amount ≥ 5); 4. Snow grain effective radius (μm); 5. Snowpack thickness (m); 6. Snowpack density (kg/m^3); 7. Albedo of underlying ground (a. Visible, 0.3–0.7 μm. b. Near-infrared, 0.7–5.0 μm); 8. MAC scaling factor (experimental) for BC; 9. BC concentration (ppb, Sulphate-coated); 10. Dust concentration (ppm, 5.0–10.0 μm diameter); 11. Volcanic ash concentration (ppm); 12. Experimental particle 1 concentration (ppb)

Date	site	1	2	3	4	5	6	7a	7b	8	9	10	11	12
14, July	C	b	79.1	b	600	0.02	378	0.15	0.3	11	129.9	56.4	0	0
14, July	D	b	67.3	b	400	0.05	289	0.15	0.3	11	77.2	29.6	0	0
15, July	A	b	78.9	b	800	0.01	289	0.13	0.12	11	608.2	649.3	0	0
15, July	B	b	75.8	b	800	0.01	289	0.13	0.12	11	657.3	3628.8	0	0
15, July	C	a	71.6	a	400	0.02	367	0.15	0.3	11	278	135.1	0	0
15, July	D	a	67.2	a	400	0.03	278	0.15	0.3	11	114	39	0	0
16, July	A	a	44.8	a	700	0.01	380	0.13	0.12	11	337	358.3	0	0
16, July	B	a	52.3	a	700	0.02	350	0.15	0.3	11	11.5	155	0	0
16, July	C	a	62.9	b	400	0.03	333	0.15	0.3	11	20.8	8.3	0	0
16, July	D	a	67.1	a	400	0.04	267	0.15	0.3	11	51.5	32.2	0	0
24, Aug	A	b	44	b	250	0.03	300	0.13	0.12	11	60.2	9.6	0	0
24, Aug	B	a	47.1	b	200	0.03	289	0.13	0.12	11	153.6	8.2	0	0
24, Aug	C	a	50.2	b	200	0.02	311	0.13	0.12	11	111.4	9	0	0
24, Aug	D	a	54.1	a	200	0.03	289	0.13	0.12	11	115.4	8.1	0	0
24, Aug	E	a	57.9	a	200	0.03	267	0.15	0.3	11	87.6	7.7	0	0
24, Aug	F	a	61.4	a	200	0.04	289	0.15	0.3	11	41.3	9.1	0	0
24, Aug	G	a	64.6	b	200	0.05	244	0.15	0.3	11	84.7	7.1	0	0
24, Aug	H	a	68.4	b	200	0.05	222	0.15	0.3	11	67.9	2.6	0	0
25, Aug	A	a	33.4	a	250	0.02	278	0.13	0.12	11	29.2	5.9	0	0
25, Aug	B	a	37.6	a	200	0.02	278	0.13	0.12	11	43.2	9.1	0	0
25, Aug	C	a	40.8	b	200	0.03	311	0.13	0.12	11	32.2	6.1	0	0
25, Aug	D	a	43.9	b	200	0.03	267	0.13	0.12	11	22.5	6.8	0	0
25, Aug	E	a	47	b	200	0.04	289	0.15	0.3	11	31.4	6.3	0	0
25, Aug	F	a	52	b	200	0.04	278	0.15	0.3	11	28.3	4.1	0	0
25, Aug	G	a	54	b	200	0.05	244	0.15	0.3	11	33.4	3.2	0	0
25, Aug	H	a	61.2	b	200	0.05	211	0.15	0.3	11	33.6	5.6	0	0
26, Aug	A	a	37.5	b	250	0.03	289	0.13	0.12	11	70.2	9.2	0	0
26, Aug	B	a	39.6	a	250	0.02	256	0.13	0.12	11	38.3	6.8	0	0
26, Aug	C	a	41.7	b	200	0.02	267	0.13	0.12	11	23	5.9	0	0
26, Aug	D	a	43.8	a	200	0.03	267	0.13	0.12	11	20.3	5.2	0	0
26, Aug	E	a	45.8	b	200	0.04	289	0.15	0.3	11	46.6	5.2	0	0
26, Aug	F	a	49.9	b	200	0.04	278	0.15	0.3	11	57.7	5.5	0	0

26, Aug	G	a	51.9	b	200	0.05	222	0.15	0.3	11	60	5.4	0	0
26, Aug	H	b	62.6	b	200	0.05	211	0.15	0.3	11	21.1	2.1	0	0

SNICAR online, http://snow.engin.umich.edu/